Yrast excitations in the neutron-rich $N = 52$ isotones

M. Czerwiński,[1] T. Rząca-Urban,[1,*] K. Sieja,[2,3] H. Sliwinska,[2,3] W. Urban,[1,4] A. G. Smith,[5] J. F. Smith,[5] G. S. Simpson,[6] I. Ahmad,[7] J. P. Greene,[7] and T. Materna[8]

[1]*Faculty of Physics, University of Warsaw, ul. Hoża 69, PL-00-681 Warszawa, Poland*
[2]*Université de Strasbourg, IPHC, 23 rue du Loess, 67037 Strasbourg, France*
[3]*CNRS, UMR7178, 67037 Strasbourg, France*
[4]*Institut Laue-Langevin, B.P. 156, F-38042 Grenoble Cedex 9, France*
[5]*Department of Physics and Astronomy, The University of Manchester, M13 9PL Manchester, United Kingdom*
[6]*LPSC, Université Joseph Fourier Grenoble 1, CNRS/IN2P3, Institut National Polytechnique de Grenoble, F-38026 Grenoble Cedex, France*
[7]*Argonne National Laboratory, Argonne, Illinois 60439, USA*
[8]*CEA Saclay, IRFU/SPHN, 91191 Gif-sur-Yvette, France*

(Received 3 April 2013; revised manuscript received 23 June 2013; published 14 October 2013)

The ^{88}Kr nucleus has been reinvestigated with prompt-γ-ray-spectroscopy methods using the Gammasphere Ge array to measure γ rays following spontaneous fission of ^{252}Cf. The order of some of the transitions, reported previously, has been changed and new levels were introduced. Angular correlation analysis allowed the assignment of spins to several levels in ^{88}Kr. These data, together with the shell-model calculations, explained the near-yrast structure of ^{88}Kr, which is similar to the structure of the $N = 52$, ^{90}Sr, and ^{92}Zr isotones. The regular systematics obtained for the three isotones suggests that the spin of the 2073.4-keV level in the ^{86}Se isotone is different from the $I = 6$ value reported previously. Using data from prompt γ-ray measurement of spontaneous fission of ^{248}Cm, we reinvestigated the ^{86}Se nucleus. A new candidate for the 6_1^+ level in ^{86}Se has been proposed, which is supported by shell-model calculations. Energies of the 2_1^+ and 4_1^+ levels in the ^{82}Zn nucleus have been predicted using a novel systematics.

DOI: 10.1103/PhysRevC.88.044314 PACS number(s): 23.20.Js, 23.20.Lv, 27.60.+j, 25.85.Ca

I. INTRODUCTION

It has been predicted by various calculations that a large excess of neutrons may significantly modify the shell structure, compared to the structure observed at the stability line [1]. The neutron-rich, doubly magic cores and nuclei around them are particularly well suited for testing such predictions. In these nuclei the nuclear excitations are expected to have simple structures, related to the well-defined single-particle levels. Therefore any change to the shell structure caused by a large excess of neutrons should be strongly manifested by changes in nuclear excitations and easy to observe.

The calculation of Ref. [1], done for neutron-rich Sn isotopes past the doubly magic ^{132}Sn core, predicts that the proton shell at $Z = 50$ may disappear, but to date there is not enough experimental evidence to verify this prediction. However, it is possible to study such effects also in other places in the nuclear chart. The very neutron-rich $^{78}_{28}$Ni$_{50}$ nucleus, expected to be doubly magic, is located significantly farther away from the stability line than any other doubly magic nucleus on the neutron-rich side. For this reason this core nucleus and its immediate neighbors may be good cases for testing the expected changes to the shell structure, caused by the neutron excess. In these nuclei one has the chance to verify the stability of both the $N = 50$ neutron shell and the $Z = 28$ proton shell when approaching ^{78}Ni [2,3]. The ultimate verification of the expected doubly magic character would be the experimental observation of excited levels in ^{78}Ni itself, which are still not accessible. However, already now it is possible to test the character of ^{78}Ni by adopting this nucleus as a doubly magic core in shell-model calculations, used to reproduce properties of nuclei in the region.

We started such studies with nuclei rather distant from ^{78}Ni, like isotopes of Zr [4], Sr [5], or Rb [6,7], which are easier to access experimentally. The reproduction of excited levels in these nuclei by large-scale shell-model calculations assuming ^{78}Ni as a core is very satisfactory and better than that by previous calculations using the ^{88}Sr nucleus as a core [8]. One would like, of course, to compare the experiment and calculations for nuclei located just above ^{78}Ni but the experimental data are more limited there and still need to be improved.

A specific question concerns the excitation energy of the 6_1^+ level in ^{86}Se and ^{88}Kr. While the 2_1^+ and 4_1^+ excitations could result from $\nu(d_{5/2})^2$, two-neutron coupling, one may expect that making a 6^+ excitation would require a promotion of one of the neutrons to the $\nu g_{7/2}$ orbit. This, however, should produce an energy gap between the 4_1^+ and the 6_1^+ excitations, as seen in ^{90}Sr and ^{92}Zr, while the value of 2073.0 keV reported previously for ^{86}Se [9] is rather small. An analogous level in ^{88}Kr is observed at 2103.9 keV [10] (though its spin is not known [10]).

In a recent work [11] a dramatic change in spin and parity, from 6^+ to 3^-, was proposed for the 2073.0-keV level in ^{86}Se. Also, the 2103.9-keV level in ^{88}Kr was assigned spin and parity 3^-, whereas higher energy levels were proposed as 6^+ excitations in both nuclei. These assignments were based on similarities to neighboring nuclei, and no specific analysis was presented to support them.

While the higher energy for 6^+ excitations is in line with the above discussion, the low position and strong population

*teresa.rzaca@fuw.edu.pl

of 3^- levels, especially in ^{86}Se, are rather unexpected. In Ref. [11] there is a call for further experimental and theoretical efforts, which are required for firm spin-parity assignments and structure explanations. In the present work we report on both experimental verification of the existing information and detailed theoretical description of $N = 52$ isotones, based on large-scale shell-model calculations. Particular effort has been devoted to spin and parity assignments and the identification of the 6^+ yrast levels in both nuclei. We used high-fold coincidence data from fission of both ^{248}Cm and ^{252}Cf. This allowed the cross-check of the reported data and revealed new interesting results, not seen in the individual measurements reported previously [9–11].

II. EXCITATIONS IN THE ^{88}Kr NUCLEUS

To improve the excitation scheme of ^{88}Kr, obtained in Ref. [10] from a measurement of prompt γ rays following spontaneous fission of ^{248}Cm, performed with the Eurogam2 array [12,13], we analyzed the data from a measurement of prompt γ rays following spontaneous fission of ^{252}Cf, performed with the Gammasphere array (see Ref. [14] for more information on the experiment). The ^{252}Cf run provided six times more triple-γ events than the ^{248}Cm measurement. Furthermore, in this work we used more advanced software [15,16], allowing searching for weak decay branches, not seen previously.

A. Level scheme of ^{88}Kr

In Fig. 1 we show a portion of the γ spectrum doubly gated in the ^{252}Cf data on known 868.8- and 1517.1-keV lines in ^{88}Kr [10]. In the spectrum there are other known lines from ^{88}Kr at 760.0 and 775.2 keV [10]. If the 760.0-1517.1-keV cascade proposed previously [10] is correct (i.e., the 1517.1-keV line above the 760.0-keV one), then the intensities of the 760.0- and 775.2-keV lines in this spectrum should be equal, because the efficiency of Ge detectors at 760.0 and 775.2 keV is nearly the same. However, the 760.0-keV line in Fig. 1 is visibly lower than the 775.2-keV line [the number of counts in the two lines is 650(42) and 820(45), respectively]. A similar effect is seen in the 775.2-868.8-1523.4-753.8-keV cascade. This can be

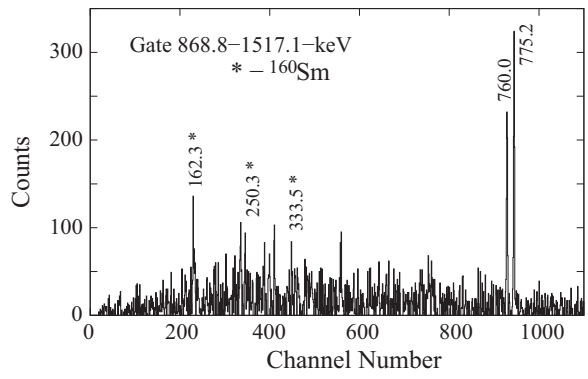

FIG. 1. γ spectrum doubly gated on the 868.8- and 1517.1-keV lines of ^{88}Kr. ^{160}Sm is a complementary fission fragment to ^{88}Kr in fission of ^{252}Cf.

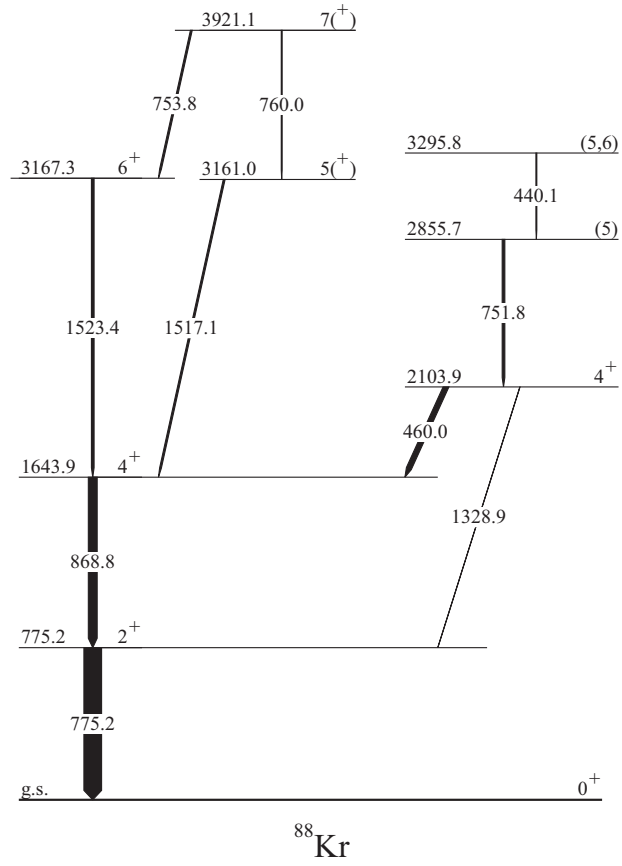

FIG. 2. Level scheme of ^{88}Kr, as deduced in this work.

understood if one places the 753.8- and 760.0-keV lines above the 1523.4- and 1517.1-keV lines, respectively, as shown in Fig. 2. A similar change in the order of these transitions was proposed in Ref. [11].

In Fig. 3 we show a portion of a γ spectrum doubly gated on the known 868.8- and 460.0-keV lines in ^{88}Kr [10]. In the spectrum a line is clearly seen at 751.8 keV and a spectrum in the inset in Fig. 3, which is doubly gated on the 751.8- and 775.2-keV lines, shows a line at 1328.9 keV, reported also in Ref. [11]). These observations and further gating indicate that the 751.8-keV line belongs to ^{88}Kr and feeds the 2103.9-keV level, a fact that has been overlooked previously [10], most likely because of lower statistics. A similar 751-753-keV doublet is reported in Ref. [11]. Consequently the intensity of the 753.5-keV doublet line seen in Ref. [10] in the 775.2-868.8-keV gate was higher than the intensity of the 1523.4-keV line in that gate, resulting in placment of the 753.5-keV line below the 1523.4-keV line in Ref. [10]. Furthermore, in Fig. 4 we show a portion of a spectrum doubly gated on the 775.2- and 868.8-keV lines of ^{88}Kr, where the 751.8 + 753.8-keV doublet and the 760.0-, 1517.1- and 1523.4-keV lines are seen. The 751.8 + 753.8-keV doublet line is clearly wider than the 760.0-keV line. We also note that the 1517.1- and 1523.4-keV groups have visible "tails." These are probably caused by the Doppler broadening (DPM effect) [17] of these lines, because of the fast decay of the 3161.0- and 3167.3-keV levels via such high-energy transitions. Consequently, a fraction of

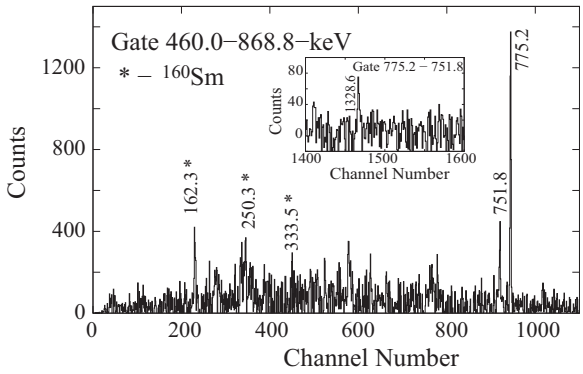

FIG. 3. γ spectrum doubly gated on the 460.0- and 868.8-keV lines of ^{88}Kr. ^{160}Sm is a complementary fission fragment to ^{88}Kr in fission of ^{252}Cf. The inset shows a portion of the γ spectrum doubly gated on the 775.2- and 751.8-keV lines of ^{88}Kr.

the intensity of the 1517.1- and 1523.4-keV transitions may be hidden in these "wings." In the previous work [10], the lower statistics prevented the observation of the two effects, leading to the underestimated intensity of the 1517.1- and 1523.4-keV transitions. Intensities of γ lines in ^{88}Kr populated in spontaneous fission of ^{252}Cf, as observed in the present work, are listed in Table I.

In Ref. [11] a number of new lines is reported, which could not be confirmed by our data. We note that the statistics in the doubly gated spectra in our work is not worse than that reported in Ref. [11], as can be seen by comparing the spectrum in Fig. 4 with the spectrum shown in Fig. 2 in Ref. [11]. Both spectra are doubly gated on the same lines. In Fig. 4 the 1517.1- and 1523.4-keV lines contain, together, 1480(75) counts. These lines, shown in Fig. 2 in Ref. [11], contain in total approximately 300 counts.

We do not confirm the 1038.9-keV transition reported in Ref. [11]. A broadened γ line of such energy is shown in Fig. 4. However, this line is, primarily, caused by the ^{70}Ge(n,n'γ) process, caused by fast neutrons accompanying fission of ^{252}Cf. In single spectra this line is very strong and is in random coincidence with all other lines, as shown in

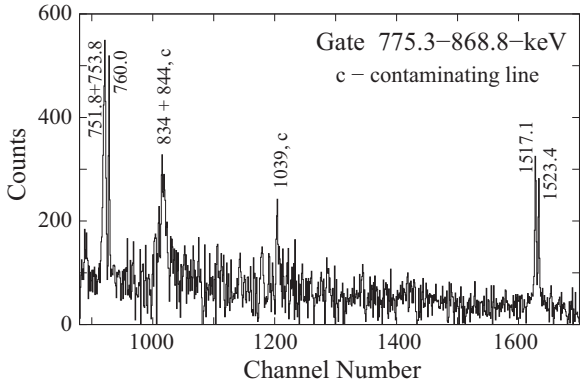

FIG. 4. High-energy portion of the γ spectrum doubly gated on the 775.2- and 868.8-keV lines of ^{88}Kr. Major unknown contaminations are labeled with a "c."

TABLE I. Energies and intensities of γ transitions in ^{88}Kr, populated in spontaneous fission of ^{252}Cf, as observed in the present work. Intensities of γ lines are in relative units.

$E_\gamma(\Delta E_\gamma)$ (keV)	$I_\gamma(\Delta I_\gamma)$ (rel.)	$E_\gamma(\Delta E_\gamma)$ (keV)	$I_\gamma(\Delta I_\gamma)$ (rel.)	$E_\gamma(\Delta E_\gamma)$ (keV)	$I_\gamma(\Delta I_\gamma)$ (rel.)
440.1(3)	5(2)	460.0(1)	24(4)	751.8(3)	10(2)
753.8(2)	8(2)	760.0(2)	7(2)	775.2(1)	100(5)
868.8(1)	76(5)	1328.9(3)	3(1)	1517.1(3)	11(2)
1523.4(3)	10(2)				

Fig. 5. Particularly strong are lines corresponding to random coincidences with other strong, single contaminating lines. Such lines originate from fast-neutron capture or scattering on the most abundant materials contained in the Gammasphere detectors: germanium, copper, and aluminum. In Fig. 5 these lines are shown at 596 keV [^{74}Ge$(n, n'\gamma)$ and ^{73}Ge(n, γ)], at 694 keV and 835 keV [^{72}Ge$(n, n'\gamma)$], and at 844 keV and 1014 keV [^{27}Al$(n, n'\gamma)$]. We note a line at 1039 keV, which is caused by random self-coincidences. Furthemore, at 772 keV there is another broad line corresponding to the ^{65}Ge$(n, n'\gamma)$ scattering. The discussed lines are broadened and skewed towards high energy, owing to the recoil, as shown in Fig. 6 in the case of the 834-, 844-, 1014-, and 1039-keV lines.

As said above, a strong contaminating line, such as the 1039-keV one, is in random coincidence with all other lines. If some of them form cascades, the contaminating line will be in coincidence with all lines in such cascades. Therefore, in a spectrum double gated on the 775.2- and 1039-keV lines there will also be a weak line at 868.8 keV. However, this is not yet a sufficient argument to place the 1039-keV line in the decay scheme of ^{88}Kr. Many double gates set in our data on the 1039-keV line and all lines below the 3921.1-keV level do not provide convincing arguments to support the presence of the 1038.9-keV transition in ^{88}Kr.

We also do not confirm the 1272.3- and 936.5-keV transitions proposed in Ref. [11]. A spectrum doubly gated on the 1039- and 1272.3-keV lines is shown in Fig. 7. Positions of lines from ^{88}Kr are marked by arrows. The "peak" at 868.8 keV contains 110(60) counts and is, most likely, caused by background fluctuation. At 753.8, 760.0, 775.2, 1517.1, and 1523.4 keV there are no peaks in our spectrum.

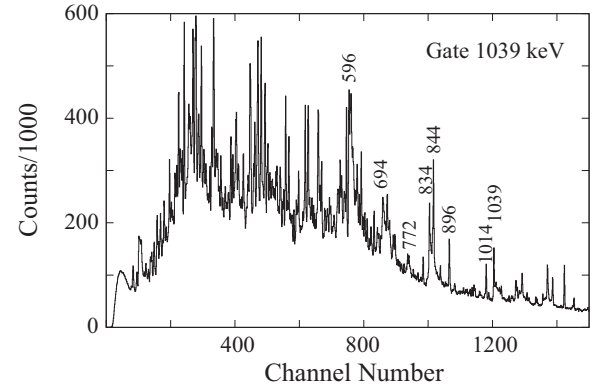

FIG. 5. A γ spectrum gated on the 1039-keV line.

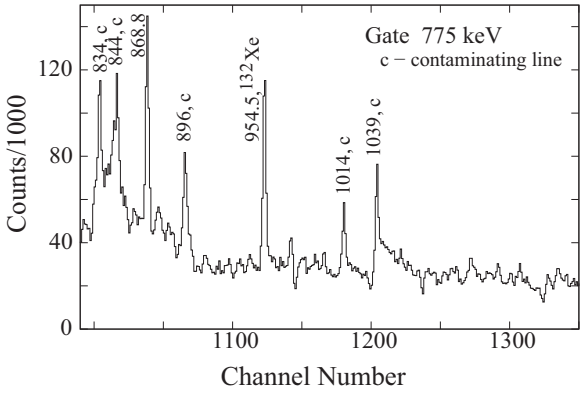

FIG. 6. A γ spectrum gated on the 775-keV line. The label "c" denotes contaminating lines owing to fast-neutron capture or scattering on germanium, copper, and aluminum, present in Ge detectors.

B. Spin and parity assignments for levels in ^{88}Kr

For the interpretation of the excited levels it is of prime importance to know their spins and parities. We have developed a technique to determine angular correlations for cascades of γ rays following spontaneous fission of ^{252}Cf and measured with Gammasphere [18], analogous to the one used for analyzing angular correlations of γ rays following spontaneous fission of ^{248}Cm measured with Eurogam2 [19]. In the present work we used this technique to extend the information on angular correlations in ^{88}Kr reported previously [10].

Of 5996 different pairs of Ge detectors present in the Gammasphere array at various angles with respect to each other, we selected six groups of such pairs, corresponding to six different values of angle Θ, defined with an accuracy of a few degrees. For each angle we sorted a $\gamma\gamma$ matrix. These six matrices were used to find intensities of various $\gamma\gamma$ cascades, at six different angles. In Fig. 8 we show examples of angular correlations obtained in this work for various $\gamma\gamma$ cascades in ^{88}Kr. To interpret experimental angular correlations we used programs developed in Refs. [18] and [20]. Solid lines represent fits to the experimental points of the angular-correlation formula

$$W(\Theta) = A_0 + A_2 \times P_2(\cos(\Theta)) + A_4 \times P_2(\cos(\Theta)),$$

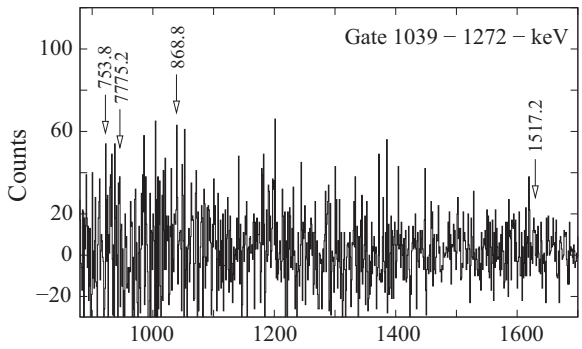

FIG. 7. A γ spectrum doubly gated on the 1039- and 1272-keV lines.

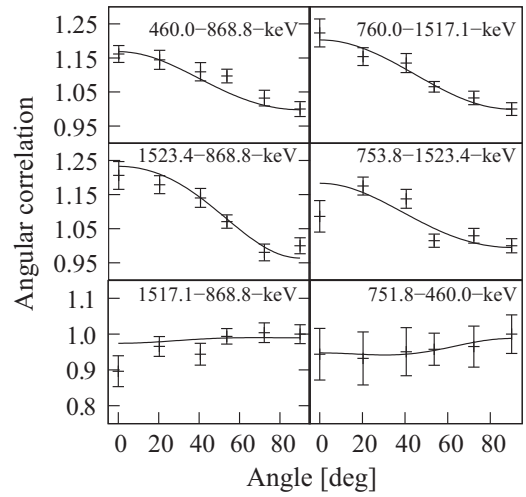

FIG. 8. Examples of angular correlations for $\gamma\gamma$ cascades in ^{88}Kr, obtained in the present work. Further details are given in the text and in Table II.

where Θ is the angle between directions of the two γ rays emitted in a cascade.

Results of the fits for $\gamma\gamma$ cascades in ^{88}Kr are listed in Table II. In Fig. 9 we show an example of the angular-correlation analysis for the 460.0-868.8-keV cascade in ^{88}Kr, where we assumed spin $I = 4$ for the 2103.9-keV level, the initial level in the cascade (the 868.8-keV transition is a stretched quadrupole). The line in the upper panel represents theoretical A_2 and A_4 values for this spin hypothesis, as a function of the mixing coefficient, δ, which varies from 0 to $\pm\infty$ along the two branches of the line, respectively. The rectangular box represents the experimental A_2/A_0 and A_4/A_0 values with their error bars. As shown there is only one solution for δ, 0.26(4). In the lower panel in Fig. 9, this is quantified in terms of the χ^2 per degree of freedom.

However, often the experimental A_4/A_0 is not accurate enough to define the unique solution. This is illustrated in Fig. 10, where we show the analysis for the 1517.1-868.8-keV cascade in ^{88}Kr. Because of the rather large error in A_4/A_0 there are two solutions, with $\delta = 0.10(3)$ and $\delta = 5.6$. Therefore, for a given cascade one may have a few possible spin hypotheses, each with one or two solutions.

Table II lists possible solutions for cascades in ^{88}Kr. To limit the number of possible solutions and propose unique spins for various levels the information from Table II should be combined with other facts, such as the observed branchings or the well-documented observation of the predominant population of yrast levels in the fission process [21]. Below we discuss this in more detail for excited levels in ^{88}Kr.

1. The 775.2- and 1643.9-keV levels

These levels, reported previously, were assigned spins and parities of 2^+ and 4^+, respectively. Our angular correlations, listed in Table II, are consistent with these spin values. Owing to the quadrupole multipolarity and the prompt character of the 775.2- and 868.8-keV transitions we interpret them as

TABLE II. Normalized experimental angular correlation coefficients for cascades of consecutive γ transitions and corresponding mixing coefficients for γ transitions in ^{88}Kr, as obtained in the present work.

Cascade E1-E2	A_{22}/A_{00}	A_{44}/A_{00}	Initial level energy, spin	δ(E1)
868.8–775.2	0.115(16)	−0.03(2)	1643.9, 2	0.17(2)
			3	0.27(3)
			3	2.16(2)
			4	0
460.0–868.8	0.105(15)	0.075(19)	2103.9, 3	−0.30(2)
			4	0.26(4)
			5	0.29(3)
			6	0
1517.1–868.8	−0.008(44)	−0.005(60)	3161.0, 4	0.55(2)
			5	0.10(3)
			5	5.6(−16, +34)
			6	0
1523.4–868.8	0.176(34)	−0.020(48)	3167.3, 4	0.06(1)
			5	0.46(11)
			6	0
760.6–1517.1	0.127(82)	0.001(110)	3921.1, 5	3.0(−22, +∞)
			6	−1.1(−13, +10)
			7	0
753.8–1523.4	0.115(68)	0.010(95)	3921.1, 5	−0.33(12)
			5	−5.4(−61, +21)
			6	0.26(26)
			6	−1.0(5)
			7	0.33(17)
			7	2.6(−9, +14)
751.8–460.0	−0.036(24)	0.020(36)	2855.5, 4	−4.0(−10, +7)
			4	0.63(7)
			5	0.06(3)
			5	6.9(−12, +17)

stretched E2 in character, which implies positive parities for the two discussed levels.

2. *The 2103.9-keV level*

Our angular correlation for the 460.0-868.8-keV cascade is consistent with four solutions for the spin of this level. Taking the stretched quadrupole multipolarity for the 868.8-keV transition we obtain for the 460.0-keV transition a mixed dipole-quadrupole character with mixing coefficient $\delta = -0.30$ when assuming spin 3 for the 2103.9-keV level, a mixed dipole-quadrupole character with mixing coefficient $\delta = 0.26(4)$ when assuming spin 4, a mixed dipole-quadrupole character with mixing coefficient $\delta = 0.29(3)$ when assuming spin 5, and a stretched quadrupole character of the 460.0-keV transition when assuming spin 6 for the 2103.9-keV level. A rather large mixing coefficient in the case of spin $I = 3$ excludes pure dipole multipolarity of the 460.0-keV transition, which therefore is not of E1 character. This excludes a negative parity for the 2103.9-keV level. Therefore we reject the 3^- spin and parity assignment for the 2103.9-keV level proposed in Ref. [11]. A spin 5 assignment for this level is unlikely, considering the observed 1328.9-keV, prompt-decay branch.

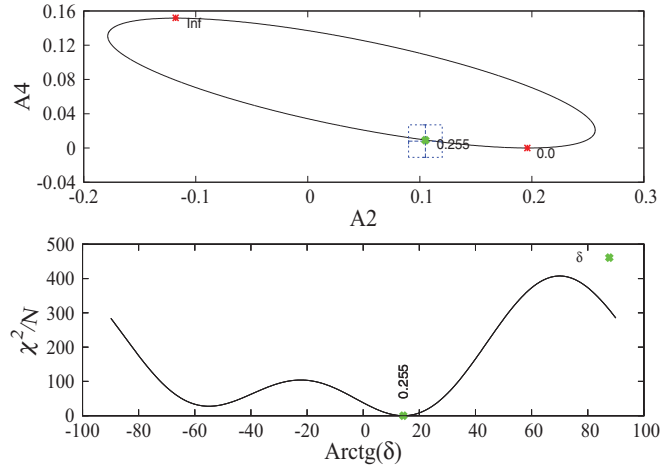

FIG. 9. (Color online) Analysis of angular correlations for the 460.0-868.8-keV $\gamma\gamma$ cascade in ^{88}Kr, performed in the present work. Further details are given in Table II and in the text.

We note that owing to the high mixing ratio for the 460.8-keV transition in the case of spin $I = 5$, this transition should have M1 + E2 multipolarity and the parity of the 2103.9-keV level should be positive. Consequently, the 1328.9-keV branch should have M3 multipolarity. This would be consistent only with a long half-life of the decaying level, which is not observed. Furthermore, the 2103.9-keV level has been also studied in β decay of ^{88}Br, where its spin was limited to 3^- or 4^+ [22], supporting the exclusion of spin 5 and spin 6. Of the two remaining solutions, spin and parity 3^+ are unlikely considering the observed branching. In the case of spin 3^+ for the 2103.9-keV level, both the 460.0-keV and the 1328.9-keV transitions should have M1/E2 character. This should favor the 1328.9-keV transition, which is not observed. Summarizing, we propose spin and parity 4^+ for the 2103.9-keV level. The positive parity is a consequence of the high mixing ratio obtained for the spin $I = 4$ hypothesis.

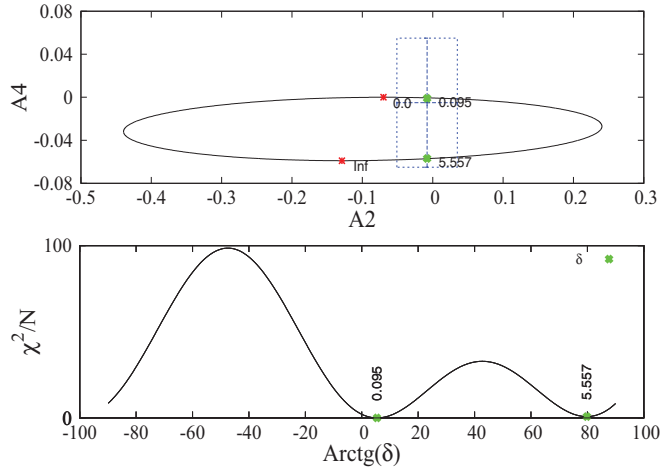

FIG. 10. (Color online) Analysis of angular correlations for the 1517.1-868.6-keV $\gamma\gamma$ cascade in ^{88}Kr, performed in the present work. Further details are given in Table II and in the text.

3. The 3161.0-keV level

The angular correlations for the 868.8-1517.1-keV cascade are consistent with three spin hypotheses for this level. Taking a stretched quadrupole multipolarity for the 868.8-keV transition we deduce for the 1517.1-keV transition a mixed dipole-quadrupole character with mixing coefficient $\delta = 0.55$ when assuming spin 4 for the 3161.0-keV level, a mixed dipole-quadrupole character with mixing coefficient $\delta = 0.10$ or 5.56 when assuming spin 5, and a stretched quadrupole character when assuming spin 6 for this level. Because there is no crossover transition between the 3161.0-keV and the 775.2-keV levels, a spin 4 assignment for this level is rather unlikely. Spin $I = 4$ would also mean a rather non-yrast character of this level, which is not favored by fission. For the spin 5 hypothesis, the nonzero mixing coefficients do not favor a pure dipole character of the 1517.1-keV transition. It is, thus, less likely to be of E1 multipolarity. Summarizing, we propose spin and parity $5^{(+)}$ or 6^+ for the 3161.0-keV level.

4. The 3167.3-keV level

The three solutions for the spin of the 3167.3-keV level, which agree with our angular correlations for the 868.8-1523.4-keV cascade are 4, 5, and 6. For the 1523.4-keV transition we obtain a mixed dipole-quadrupole character with mixing coefficient $\delta = 0.06$ when assuming spin 4, a mixed dipole-quadrupole character with mixing coefficient $\delta = 0.46$ when assuming spin 5, and a stretched quadrupole character when assuming spin 6 for the 3167.3-keV level. A spin 4 assignment for this level is unlikely because there is no observed decay from the 3167.3-keV level to the 775.2-keV level. For the spin 5 hypothesis, the nonzero mixing coefficients exclude a pure dipole character of the 1517.1-keV transition. Therefore it is unlikely to be an E1 transition. Concluding, we propose spin and parity $5^{(+)}$ or 6^+ for the 3167.3-keV level.

5. The 3921.1-keV level

We note that because of the small difference between the excitation energy of the 3161.0-keV and that of the 3167.30-keV level, it is unlikely that they have the same spin and parity. Therefore one of them should have spin and parity $5^{(+)}$, and the other spin and parity 6^+. In this case spin 8 for the 3921.1-keV level can be excluded, considering the observed decay branchings for this level. There still remains an ambiguity: which of the two levels has spin $5^{(+)}$ and which has spin 6^+. This can be resolved with our angular correlations. For the two alternatives we performed fits to the experimental angular correlations of the 1517.1-760.0- and 1523.4-753.8-keV cascades. A better fit was obtained when assuming spin 6^+ for the 3167.3-keV level with a stretched quadrupole character of the 1523.4-keV transition and spin $5^{(+)}$ for the 3161.0-keV level with a mixed dipole-quadrupole character of the 1517.1-keV transition, with mixing coefficient $\delta = 0.10$. With these assumptions we have found that there are three solutions, $I = 5$, 6, and 7, for the spin of the 3921.1-keV level, which agree with angular correlations for the 1517.1-760.0- and 1523.4-753.8-keV cascades. For the 753.8-keV transition a dipole-quadrupole solution with $\delta = -0.33$ is obtained when assuming spin 5 for the 3921.1-keV level, a dipole-quadrupole character with mixing coefficient $\delta = 0.26$ when assuming spin 6 for the 3921.1-keV level, and a dipole-quadrupole character with mixing coefficient $\delta = 0.33$ when assuming spin 7 for the 3921.1-keV level. For the 760.0-keV transition we obtain a dipole-quadrupole character with mixing coefficient $\delta = 3.0$ for spin 5 of the 3921.1-keV level, a dipole-quadrupole character with mixing coefficient $\delta = -0.17$ when assuming spin 6, and a stretched quadrupole character when assuming spin 7 for the 3921.1-keV level. The large mixing coefficients exclude a pure dipole character of the 753.8-keV transition, which therefore is not of E1 character. Consequently, negative parity for the 3921.1-keV level is excluded. We also do not observe a direct decay from the 3161.0- to the 1643.9-keV level. For these reasons spin 5 or 6 assignments for the 3921.1-keV level are rather unlikely. Concluding, we propose spin and parity $7(^+)$ for the 3921.1-keV level. We note that our proposition of a positive parity for the 3161.0- and 3921.1-keV levels differs from the proposition in Ref. [11], where negative parity was proposed for these levels.

6. The 2855.7-keV level

For the 460.0-751.8-keV cascade our angular correlations are consistent with two solutions for the spin of this level: $I = 4$ and 5. In the analysis we assumed that the 460.0-keV transition is of dipole-quadrupole character with mixing coefficient $\delta = 0.26$ as discussed above. High mixing ratios associated with the spin 4 hypothesis (see Table II) indicate a positive parity for the 2855.7-keV level. However, a spin 4 solution is less likely, because we do not observe a crossover decay from the 2855.7-keV level to the 1643.9-keV level. Another argument against the spin 4 hypothesis is the fact that in this case the 2855.7-keV level would be rather non-yrast, while the population of such levels in the fission process is less likely. Therefore, we tentatively propose spin 5 for the 2855.7-keV level.

7. The 3295.8-keV level

No angular correlations could be measured for the 440.1-751.8-keV cascade. From the yrast-population argument, spin 5 or 6 may be considered for this level.

III. EXCITATIONS IN THE ^{86}SE NUCLEUS

Yrast excitations in ^{86}Se have been reported up to spin 6^+ from the study of prompt-γ radiation following spontaneous fission of ^{252}Cf [9]. Convincing arguments were presented to support the presence of the 704.1- and 863.4-keV transitions and the 1567.6-keV second excited level in ^{86}Se. However, the evidence for the 505.5-keV decay of the 6^+ level in Ref. [9] is rather weak (see Fig. 4(b) in Ref. [9]). We also note that

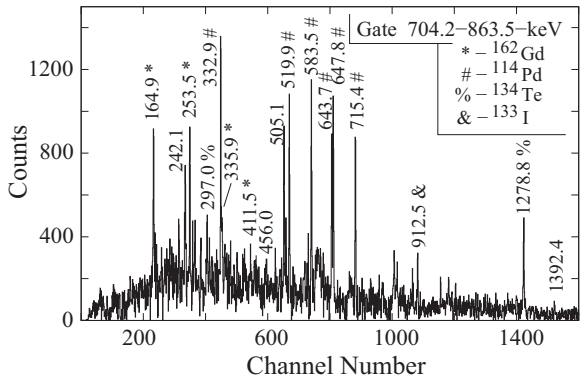

FIG. 11. γ spectrum doubly gated on the 704.2- and 863.4-keV lines of ^{86}Se. ^{162}Gd is the most pronounced complementary fission fragment to ^{86}Se in spontaneous fission of ^{252}Cf.

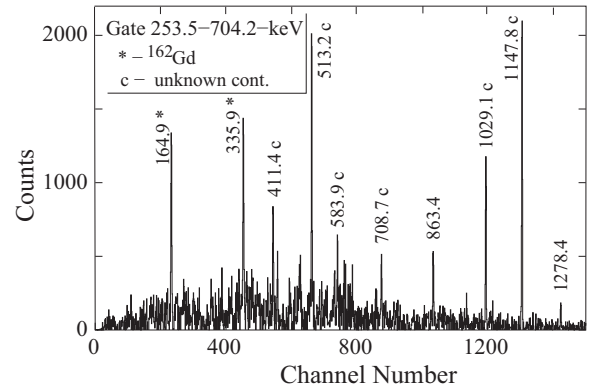

FIG. 12. γ spectrum doubly gated on the 253.5-keV line of ^{162}Gd and the 704.2-keV line of ^{86}Se, in the ^{252}Cf fission data.

no arguments were given to support the 6^+ spin and parity assignment for the 2073.4-keV level in Ref. [9]. In Ref. [11] the spin and parity assignment for the 2073.4-keV level has been changed from 6^+ to 3^-, but, again, without quantitative arguments. The assignment was made based on the similarity to heavier $N = 52$ isotones. But as we have shown above the spin and parity of the 2103.9-keV level in ^{88}Kr is not 3^- and the systematics proposed in Ref. [11] breaks.

In the present work we have reinvestigated the discussed cascade in ^{86}Se in order to verify the presence of the 505.5-keV transition and, more importantly, to search for another candidate for the 6_1^+ level, which would be consistent with the picture seen in the heavier $N = 52$ isotones. To study ^{86}Se we have used triple-γ coincidences from spontaneous fission of ^{252}Cf [14], as described above, as well as triple-γ coincidences from spontaneous fission of ^{248}Cm, measured using the Eurogam2 array [12,13].

In Fig. 11 we show a spectrum doubly gated on the 704.2- and 863.4-keV lines of ^{86}Se from the ^{252}Cf Gammasphere data. Clearly shown in the spectrum are lines of ^{162}Gd, the most pronounced complementary fragment to ^{86}Se, corresponding to emitting 4 neutrons in spontaneous fission of ^{252}Cf. Strong contaminating lines from ^{114}Pd are present because ^{114}Pd has the 703.9- and 862.9-keV transitions in its ground-state cascade. Owing to the fact that ^{114}Pd is the strongest fission-fragment partner to ^{134}Te in fission of ^{252}Cf, there are also 1278.8- and 297.0-keV lines of ^{134}Te. In the spectrum there is a pronounced line at 505.4 keV, in accord with Ref. [9]. However, in the spectrum doubly gated on the 704.2-keV line of ^{86}Se and the 253.5-keV line of ^{162}Gd, shown in Fig. 12, the 505.4-keV line is barely seen. This also coincides with Ref. [9], where, in their Fig. 4(b), the 505-keV line is surprisingly weak. These observations could be explained assuming that the 505.4-keV decay depopulates a level in ^{86}Se which is populated strongly in β decay of ^{86}As, produced in fission. In the present ^{252}Cf Gammasphere data the time window was about 900 ns long and a substantial number of events corresponding to β decay of fission products and their daughter nuclei have been collected apart from prompt-γ events.

This conclusion is consistent with the spectrum shown in Fig. 13, which is doubly gated on the 505.4- and 863.4-keV lines. The spectrum is dominated by the 704.2-keV line of ^{86}Se (consistent with the strong population in β decay), while lines from the ^{162}Gd complementary fragment are rather weak. It should be mentioned, however, that some prompt feeding in fission of the 2073.0-keV level is likely. In the spectrum shown in Fig. 13 we observe a new line at 989.5 keV. In a spectrum shown in Fig. 14, which is doubly gated on this new line and the 505.4-keV line, both 704.2- and 863.4-keV lines of ^{86}Se are seen, suggesting that the new, 989.5-keV line corresponds to a prompt-γ feeding of the 2073.0-keV level.

In the spectrum shown in Fig. 12 there is a line at 1278.4 keV. A spectrum doubly gated of the 1278.4- and 863.4-keV lines, shown in Fig. 15, reveals a strong 704.2-keV line of ^{86}Se and weak lines of ^{162}Gd. Contaminating lines from ^{114}Pd at 332.9 and 519.9 keV and a weak 297.0-keV line from ^{134}Te derive from the ^{114}Pd-^{134}Te coincidence, as shown previously in Fig. 11. However, in Fig. 15 the 704.2-keV line of ^{86}Se clearly dominates (we note that this line is different from the 706.3-keV line of ^{134}Te). Therefore one may assume that the 1278.4-keV line shown in Fig. 15 belongs to ^{86}Se and is not entirely caused by the 1278.8-keV contamination from ^{134}Te.

To verify this important conclusion we gated on triple-γ coincidences from the ^{248}Cm fission data collected with Eurogam2, where the ^{114}Pd-^{134}Te coincidence is not present. In Fig. 16, obtained from these data, one observes the

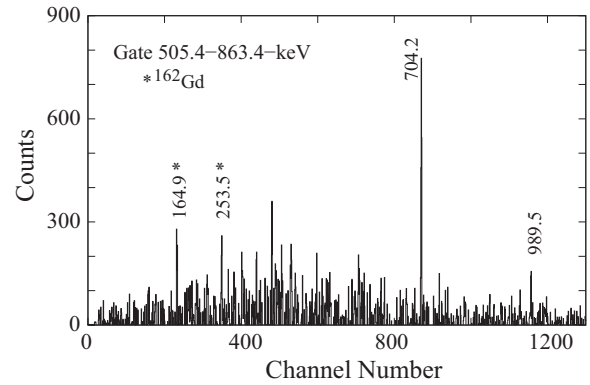

FIG. 13. γ spectrum doubly gated on the 505.4- and 863.4-keV lines of ^{86}Se, in the ^{252}Cf fission data.

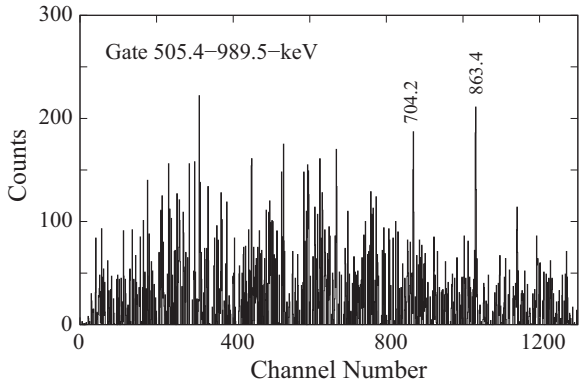

FIG. 14. γ spectrum doubly gated on the 505.4-keV line of ^{86}Se and the new 989.5-keV line in the ^{252}Cf fission data.

704.2-keV line of ^{86}Se and lines of ^{158}Sm, the most pronounced complementary fission fragment to ^{86}Se in fission of ^{248}Cm. The 297.0-keV line from ^{134}Te is not seen here, which means that the 1278-keV gate is not contaminated by the 1278.8-keV line of ^{134}Te and contains only the 1278.4-keV line of ^{86}Se. This transition, feeding the 1567.6-keV level in ^{86}Se, defines a new level in ^{86}Se at 2846.0 keV.

Interestingly, in both, Figs. 15 and 16, there is a new line at 456.0 keV. A spectrum double-gated on the 1278.4- and 456.0-keV lines, shown in Fig. 17, shows weak evidence of the 704.2- and 863.4-keV lines of ^{86}Se in this gate. Therefore, we propose a new level at 3302.0 keV, depopulated by the 456.0-keV transition.

The excitation scheme of ^{86}Se, based on the coincidences discussed above, is shown in Fig. 18. Relative intensities of γ lines are given in brackets next to their energies (in keV). Three levels, at 2846.0, 3062.5, and 3302.0 keV, in ^{86}Se are rather certain. Because of the weak evidence for the 456.0-keV line in Fig. 18 the 3302.0-keV level is introduced only tentatively.

In Ref. [11] some other lines were proposed which are not confirmed in this work. We do not observe the 1465-keV transition, neither in our ^{252}Cf nor in our ^{248}Cm data. Consequently, we cannot confirm the 3033-keV level proposed in Ref. [11]. We also do not confirm the 706-1027-1014-keV cascade or the 3768-, 4769-, and 5810-keV levels proposed Ref. [11].

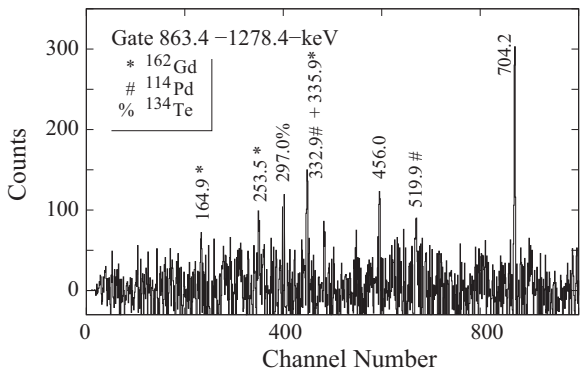

FIG. 15. γ spectrum doubly gated on the new 1278.4-keV line and the 863.4-keV line of ^{86}Se in the ^{252}Cf fission data.

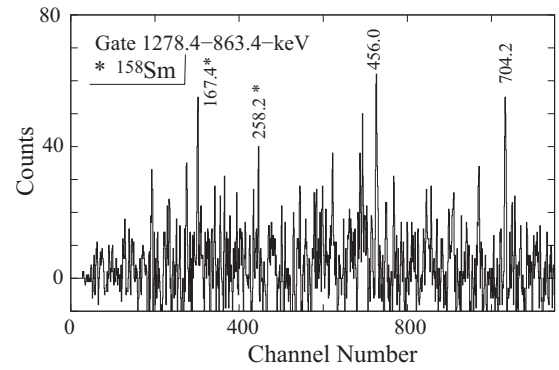

FIG. 16. γ spectrum doubly gated on the new 1278.4-keV line and the 863.4-keV line of ^{86}Se in the ^{248}Cm fission data.

Angular correlation determined in the present work for the 704.2-863.4-keV cascade, with $A_2/A_0 = 0.097(12)$ and $A_2/A_0 = 0.014(16)$, is consistent with both lines having stretched quadrupole multipolarity. However, one should remember that this cascade is contaminated by the 703.8-862.4-keV cascade of two transitions, most likely of stretched quadrupole character, present in the ground-state band of ^{114}Pd. Other lines of ^{86}Se seen in this work are too weak for angular correlation analysis.

Taking into account the argument of a yrast population in the fission process, the observed γ intensities and the fact that the 2073.0-keV level is at least partly populated in β decay of ^{86}As, we propose that the spin of the 2073.0-keV level is lower than 6. By analogy with ^{88}Kr one may propose spin and parity 4^+ for this level. For the new level at 2846.0 keV we propose, tentatively, spin and parity 6^+, using the argument of yrast populating in fission and the similarity to ^{88}Kr. However, spin 5 for the 2846.0-keV level cannot be excluded. For the 3063.5-keV level we propose, tentatively, spin 5 or 6, taking into account its population and decay branches.

IV. DISCUSSION

The $N = 52$ isotones are expected to be spherical nuclei with excitations dominated by single-particle couplings plus some admixture of collective motion. At low excitation

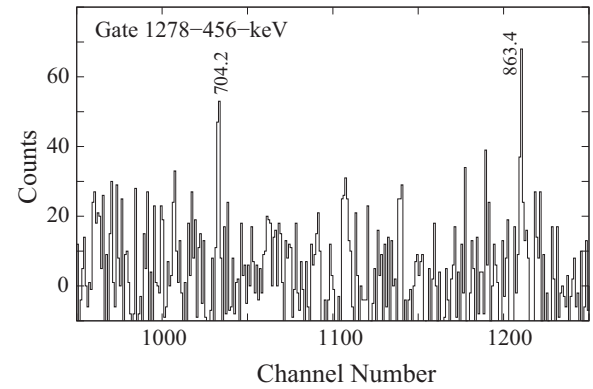

FIG. 17. γ spectrum doubly gated on the new 1278.4- and 456.0-keV lines in the ^{248}Cm fission data.

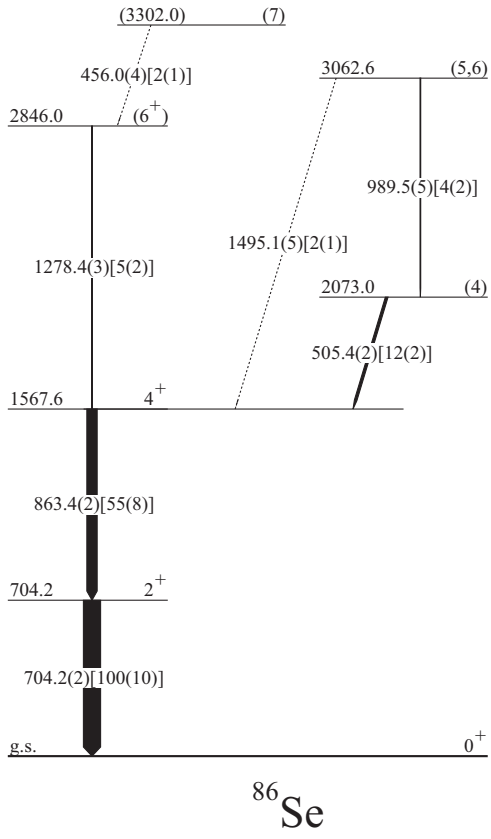

FIG. 18. Level scheme of ^{86}Se, as deduced in the present work. Intensities of γ lines are shown in brackets.

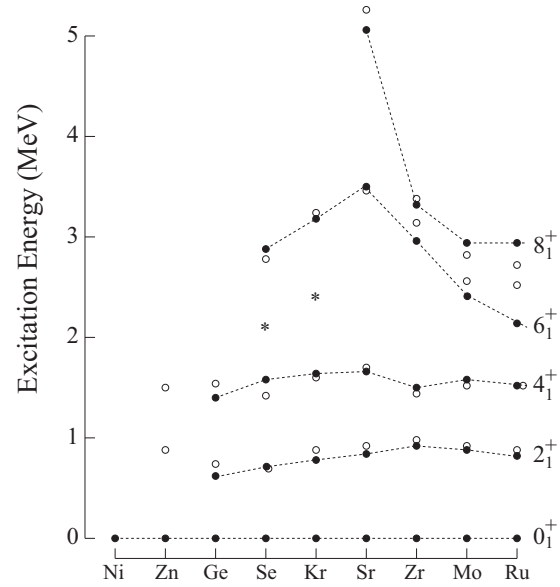

FIG. 19. Systematics of excitation energies of yrast levels in $N = 52$ isotones (filled circles). Data are taken from the present work and from Refs. [9,10], and [23–27]. Open circles represent energies obtained in the present shell-model calculations. Asterisks represent experimental energies of the 6_1^+ level in ^{86}Se and ^{88}Kr, reported previously [9,10].

energies the two valence neutrons occupy the $d_{5/2}$ orbital, where they can couple and contribute to levels with spin 0^+, 2^+, and 4^+. At higher energies one or both of these neutrons can be promoted to another orbital (e.g., $g_{7/2}$) and produce levels with spin 6^+ and higher. One may also think of coupling to a proton pair. Such processes would require extra energy and one may expect an increased energy gap between the 4^+ and the 6^+ levels. This can be seen in the systematics of excitation energies of yrast levels in the $N = 52$ isotones, shown in Fig. 19. With the new energies of the 6^+ levels in ^{86}Se and ^{88}Kr, which are comparable to those observed in ^{90}Sr and ^{92}Zr, a clear energy gap between the 4^+ and the 6^+ levels is observed in these nuclei. The asterisks in Fig. 19 show the positions of the 6^+ levels in ^{86}Se and ^{88}Kr, reported previously [9,10].

Thus, in the first approximation, the discussed excitations can be explained by the coupling of two valence neutrons. This simplified interpretation is, however, modified by the presence of valence protons and their interaction with neutrons. While the energies of the 2^+ and 4^+ levels only weakly depend on the proton number, the energy of the 6^+ level shows significant variations. First, it grows with the proton number to about 3.4 MeV in ^{90}Sr. This can be associated with the $Z = 38$ subshell closure. Up to $Z = 38$ the trend of 6^+ energy reflects the behavior of 2^+ states in $N = 50$ isotones, which suggests that the 6^+ level can be formed as a coupling of two aligned neutrons to the proton 2^+. Afterwards the 6^+ excitation energy drops quickly. It is somewhat surprising to observe this decrease already for ^{92}Zr, where another subshell closure is present at $Z = 40$, as manifested in the excitation energies of the 2^+ and 4^+ levels in ^{90}Zr. This indicates another mechanism contributing to the 6^+ excitation energy above $Z = 38$. A possible explanation is the population of the $g_{9/2}$ proton orbital in nuclei with $Z \geqslant 40$. It is predicted that the $g_{9/2}$ proton interacts strongly with the $g_{7/2}$ neutron, its spin-orbit partner. The spin-orbit-partner mechanism has been proposed as one of the effects producing strong quadrupole deformation in neutron-rich nuclei around $Z = 40$ [28,29], which was recently verified for Ru isotopes [30].

In the present work we do not confirm spin and parity 3^- for the 2073- and 2104-keV levels in ^{86}Se and ^{88}Kr, respectively, as proposed in Ref. [11]. These and a few other levels, reported in Ref. [11] with negative parity, were assigned positive parity in this work. Thus, the dominance of low-energy negative-parity excitations proposed in Ref. [11], which might suggest an enhanced octupole collectivity in the $N = 52$ isotones, is not confirmed.

A. Calculations

To obtain deeper insight into the structure of the yrast excitations in $N = 52$ isotones, and to verify the approximate interpretation proposed above, we have performed shell-model calculations with a large valence space including $(1f_{5/2}, 2p_{1/2}, 2p_{3/2}, 1g_{9/2})$ orbitals for protons and $(2d_{5/2}, 3s_{1/2}, 2d_{3/2}, 1g_{7/2}, 1h_{11/2})$ orbitals for neutrons outside the ^{78}Ni nucleus used as the inert core. Such a valence space, adopted in a number of our previous studies in this region for various Zr, Y, Sr, and Rb isotopes [4–7], has been proven

successful and clearly better for description of the observed low-energy excitations than the one outside the ^{88}Sr core proposed in earlier calculations [8]. The effective interaction used in this work was derived by the monopole corrections of realistic G matrices based on the CD-Bonn potential. A broader discussion of the interaction and its other applications can be found in Ref. [4].

The calculations were performed using the m-scheme shell-model code ANTOINE [31] and, in several cases, the coupled-scheme code NATHAN [32]. The size of matrices for the $N = 52$ nuclei in the considered valence space does not exceed 3×10^6 in the m scheme, thus, full space diagonalizations are feasible and the computations are not at all time-consuming. This is an important advantage of the ^{78}Ni core, when studying exotic nuclei located above it. Therefore, further development of interactions in the proposed valence space and experimental probing of the single-particle structures in the vicinity of ^{78}Ni are particularly interesting for future shell-model applications.

Excitation energies of yrast levels in ^{82}Zn, ^{84}Ge, ^{86}Se, ^{88}Kr and ^{90}Sr, ^{94}Mo, ^{96}Ru, calculated in this work, and in ^{92}Zr, calculated previously [4], are compared to the experimental excitation energies in Fig. 19. The reproduction of the experimental data is very good in the excitation energy range up to 5 MeV. Particularly satisfying is the reproduction of the largely varying energy gap between the 4_1^+ and the 6_1^+ levels. The wave functions of these two levels obtained from shell-model diagonalizations reveal that the two valence neutrons are preferably confined in the $d_{5/2}$ orbital (average occupancy, $\geqslant$1.5 nucleon) for all nuclei. The coupling of 0_p^+ to 4_n^+ is the preferred component in the 4^+ states: 55% in Ge, 47% in Se, 70% in Kr, 83% in Sr and 91% in Zr, 76% in Mo, 63% in Ru. Because the two neutrons in the $d_{5/2}$ orbital can be coupled to a maximum spin of 4^+, the 6^+ has to have a different structure than the 4^+. One of the possibilities is coupling of a neutron 4_n^+ to a proton 2_p^+. The $2_p^+ \otimes 4_n^+$ component is indeed dominating (or significant) up to $Z = 38$, with 67% in Ge, 81% in Se, 30% in Kr, and 90% in Sr. While for $Z \leqslant 38$ the 2^+ proton can be formed by particles in $p_{3/2}$ and $f_{5/2}$ orbitals, in ^{90}Sr at least one particle has to be promoted to $p_{1/2}$, owing to the filling of the $f_{5/2}$ and $p_{3/2}$ levels. This costs extra energy and causes a rise in the 6^+ level. Therefore, up to $Z = 38$ the trend of 6^+ states reflects very well the behavior of 2^+ states in $N = 50$ nuclei. Based on this observation, one may conclude that shell-model wave functions favoring a $2_p^+ \otimes 4_n^+$ component have a realistic character. Past the $Z = 38$ subshell, the calculated 6^+ changes its structure and contains 50% of the $6_p^+ \otimes 0_n^+$ configuration in the wave function of Zr, with two protons occupying the $g_{9/2}$ orbital. *A priori*, in Zr one can expect a similar behavior as in Sr, owing to the $p_{1/2}$ shell closure. Nevertheless, the occupation of the $g_{9/2}$ orbital is significant already in the ground state of Zr (1.5 particle), thus no considerable extra energy is required to form the proton 6^+, which is lowered in energy with respect to Sr. The same structure, i.e., $6_p^+ \otimes 0_n^+$, dominates in the 6^+ of Mo and Ru, with 57% and 42%, respectively.

We have also calculated several non-yrast levels in the discussed nuclei. In Fig. 20 we compare the experimental 0_2^+, 2_2^+, and 4_2^+ levels with their theoretical counterparts, calculated with the shell model using the same interaction. The data for

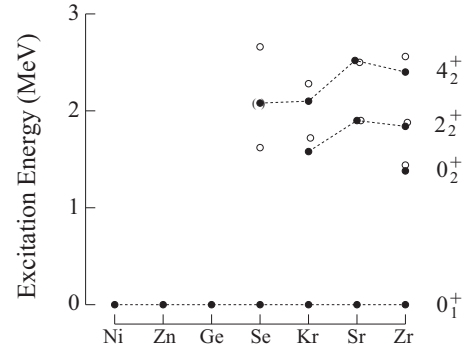

FIG. 20. Excitation energies of 0_2^+, 2_2^+, and 4_2^+ levels in $N = 52$ isotones (filled circles). Data are taken from the present work and from Refs. [9,10], and [23–27]. Open circles represent energies obtained in shell-model calculations performed in this work for ^{86}Se, ^{88}Kr, and ^{90}Sr. Calculated energies for ^{92}Zr are taken from Ref. [4].

the ^{90}Sr and ^{92}Zr are taken from Refs. [24] and [25]. The reproduction of the experiment by the shell model is good. The calculated levels follow the trend of experimental points when changing the proton number and there is a clear distinction between various spins. In particular, the calculations support the 4_2^+ spin and parity assigned to the 2130.9-keV level in ^{88}Kr. However, for the 4_2^+ level in ^{86}Se, proposed tentatively at the 2073.0-keV level, the calculated energy is clearly different. It is of great interest to identify experimentally the 2_2^+ level in ^{86}Se, to check how the shell model performs there. This may help to verify whether the observed discrepancy requires improved calculations or if the spin assignment to the 2073.0-keV level is not correct. As discussed below, the structure of the 2_2^+ and 4_2^+ levels in $N = 52$ isotones is different from the structure of their yrast counterparts. Therefore their further investigation may be useful.

In Fig. 21 we show also other non-yrast levels, experimental and calculated, in ^{88}Kr. One may note that there are theoretical partners for all the experimental positive-parity levels. As already noted in the case of even-even Sr isotopes [5], the 3^- level is not well reproduced by the shell model in this region. The proper description of 3^- levels, which are of an octupole collective nature, requires the superposition of contributions from many $\Delta l = 3$ levels, probably beyond the current model space. There are also a number of higher spin, near-yrast levels with negative parity predicted by our calculations. It is of interest to search experimentally for these levels. In even-even Sr isotopes higher-spin, negative-parity levels were reproduced rather well by the calculations [5].

Let us now inspect in more detail the wave functions predicted by our calculations in ^{88}Kr. The corresponding occupation numbers for proton and neutron orbitals are listed in Table III. The population of various orbitals in ^{88}Kr is rather similar for all the yrast levels discussed, from 0_1^+ to 7_1^+. The only exception is the lowering of the population of the $\nu s_{1/2}$, $\nu d_{3/2}$, and $\pi p_{1/2}$, low-j orbitals with increasing spin. However, this seems to be a secondary effect, compared to the population of the strongly occupied orbitals, $\nu d_{5/2}$, $\pi f_{f/2}$, and $\pi p_{3/2}$, which does not change with spin. Furthermore, the population of high-j orbitals $\nu h_{11/2}$ and $\pi g_{9/2}$ is small

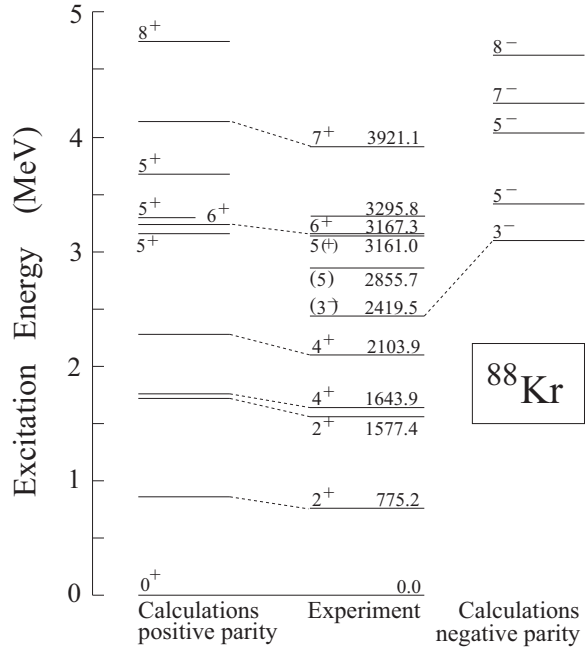

FIG. 21. Comparison of the shell-model calculations for ^{88}Kr with the experimental data, both obtained in the present work. The 1577.4- and 2419.5-keV experimental levels are taken from Ref. [22].

and decreases with spin. To better understand the structure of these states, we have therefore analyzed the couplings of the underlying proton and neutron subspaces. The yrast levels 2^+ and 4^+ are predominantly caused by the coupling of two neutrons in the 2^+_n and 4^+_n states, respectively, with the proton 0^+_p. The non-yrast 2^+_2 and 4^+_2 states, though having the same occupancies as the yrast ones, appear to be of a different structure. The 2^+_2 is more complex than 2^+_1 and contains 24% $0^+_p \otimes 2^+_n$, 34% $2^+_p \otimes 0^+_n$, and 33% $2^+_p \otimes 2^+_n$. The 4^+_2, contrary to the 4^+_1, is of a proton origin; i.e., its wave function is dominated by the $4^+_p \otimes 0^+_n$ component (48%). It is interesting to note that the 6^+ state of ^{88}Kr appears more mixed than the 6^+ in the remaining $N = 52$ isotones with $Z \leqslant 38$. The $2^+_p \otimes 4^+_n$ configuration is as probable (30%) as the $4^+_p \otimes 2^+_n$ (35%) and $4^+_p \otimes 4^+_n$ (27%). The wave function of the 7^+ comes from the coupling of $4^+_p \otimes 4^+_n$ (88%).

TABLE III. Occupation of various neutron and proton orbitals, as calculated in this work for levels in ^{88}Kr.

	Level						
	0^+_1	2^+_1	2^+_2	4^+_1	4^+_2	6^+_1	7^+_1
				Neutrons			
$d_{5/2}$	1.66	1.71	1.50	1.85	1.71	1.86	1.88
$s_{1/2}$	0.09	0.13	0.34	0.04	0.08	0.04	0.03
$g_{7/2}$	0.09	0.07	0.09	0.07	0.09	0.06	0.06
$d_{3/2}$	0.07	0.04	0.05	0.10	0.05	0.02	0.01
$h_{11/2}$	0.08	0.05	0.05	0.03	0.07	0.03	0.02
				Protons			
$f_{5/2}$	4.26	4.22	4.23	4.38	4.62	4.68	4.73
$p_{3/2}$	2.74	2.73	2.68	2.66	2.61	2.70	2.71
$p_{1/2}$	0.61	0.69	0.80	0.57	0.52	0.37	0.32
$g_{9/2}$	0.39	0.36	0.30	0.39	0.25	0.26	0.24

We have also calculated branching ratios in ^{88}Kr and here the calculations seem to perform worse. The calculated E2 decay rate from the 6^+_1 level to the 4^+_2 level is nearly as high as that to the 4^+_1, which is not seen in the experiment. Also, the calculated E2 decay rates from the 4^+_2 level to the 2^+_1 and 2^+_2 levels are higher than that to the 4^+_1, in contrast to what is observed experimentally. Taking into account, in the calculations, the M1 component improves the situation, but not sufficiently. The wave functions of the yrast and non-yrast 4^+ states should be more mixed to enhance the transition probability between them. Unfortunately, it is difficult to state which part of the effective interaction could amplify the mixing of different components, preserving, at the same time, the accurately reproduced energies of these levels.

B. Systematic predictions for ^{82}Zn

The systematic prediction of excitation energies in $N = 52$ isotones, shown in Fig. 19, can be used to predict excitations in the ^{82}Zn nucleus. A simple extrapolation of the observed trends suggests that the excitation energies of the 2^+ and 4^+ levels in ^{82}Zn are lower than in ^{84}Ge. On the other hand, if the $Z = 28$ proton closure is still maintained at $N = 52$, one may expect that the 2^+ level in ^{82}Zn has a higher excitation energy than in ^{84}Ge, by analogy to the situation observed in $N = 84$ isotones. For illustration, Fig. 22(a) compares excitations in $N = 52$ isotones (filled circles) to analogous excitations in $N = 84$ isotones (squares).

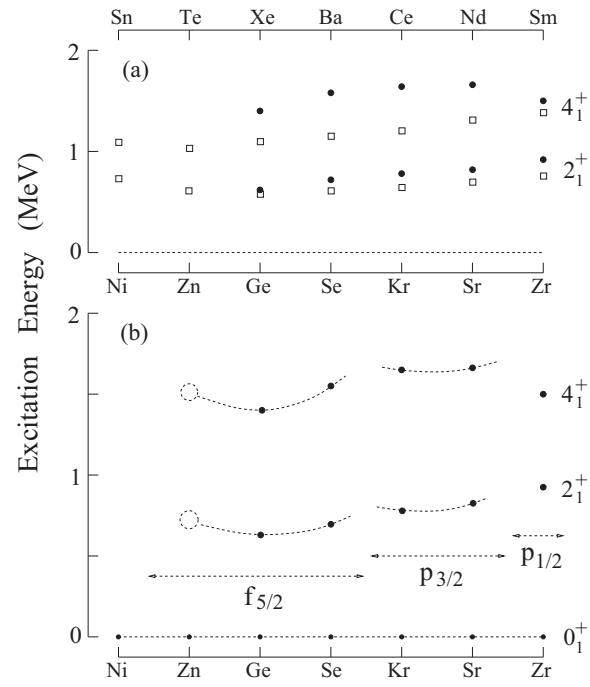

FIG. 22. (a) Systematics of 2^+_1 and 4^+_1 excitations in $N = 52$ and $N = 84$ isotonic chains. (b) Novel systematics of 2^+_1 and 4^+_1 excitations in $N = 52$ isotones. See text for further discussion.

We would like to propose another systematic estimate for the excitation energies of the 2^+ and 4^+ levels in ^{82}Zn based on the observation of certain regularities connected with filling of subshells. In our previous work on neutron-rich Pd [33] and Ru [34] nuclei we have shown that systematics of excitation energies as a function of neutron number in Mo, Ru, and Pd isotopes can be linked to the filling of subsequent subshells. A more comprehensive study of subshell effects on collectivity can be found in a recent review by Heyde and Wood [35].

It is a well-established fact that the collective effects in nuclei are at their maximum around the middle of a shell. For example, the 2_1^+ excitation energy in even-even nuclei reaches its minimum. This is documented in general in Ref. [36] and in the case of Ru and Pd in Ref. [37] and also in Fig. 7 in Ref. [33]. One may expect that, on a smaller scale, a similar effect may also be observed within individual subshells of the major shell. This is indeed seen in the systematics of the 2_1^+ excitation energy in even-even Mo, Ru, and Pd isotopes (see Fig. 7 in Ref. [33]).

In $N = 52$ isotones, above the $Z = 28$ closed shell, protons can occupy the $f_{5/2}$, $p_{3/2}$, and $p_{1/2}$ orbitals. It is now accepted that they first populate the $f_{5/2}$ orbital and the $p_{3/2}$ orbital [2,3,23,38–41]. In Fig. 22(b) we show excitation energies of the 2^+ and 4^+ levels in $N = 52$ isotones and sketch the systematic dependence (dashed lines) analogous to those in Refs. [33] and [34]. The shapes of these dependences are, somewhat arbitrarily, assumed to be parabola-like, with minima in the middle of the respective subshells. Assuming that the minimum of the 2^+ and 4^+ excitation energies, connected with the filling of the $f_{5/2}$ orbital, is reached at ^{84}Ge, we propose that the excitation energy of the 2^+ and 4^+ levels in ^{82}Zn are about 750 and 1500 keV, respectively, which is in good agreement with the shell-model predictions shown in Fig. 19. These values may be helpful when searching experimentally for excitations in this nucleus.

V. SUMMARY

In the present work we have studied experimentally the yrast and near-yrast levels in the $N = 52$ isotones, ^{88}Kr and ^{86}Se, populated in spontaneous fission of ^{252}Cf and ^{248}Cm. In both nuclei we have proposed new 6_1^+ levels, which fit well the systematics of such levels in $N = 52$ isotones, where a characteristic energy gap is observed between 4_1^+ and 6_1^+. The 2073-keV level in ^{86}Se, reported previously as the 6_1^+ excitation, has been assigned spin and parity 4^+ in this work. A similar assignment has been made for the 2103.9-keV level in ^{88}Kr. We have performed large-scale shell-model calculations for excited levels in the $N = 52$ isotones with $30 \leqslant Z \leqslant 44$. The calculations reproduce very well the yrast excitations in the four $N = 52$ isotones, confirming, in particular, the 4_1^+–to–6_1^+ energy gap. This agreement confirms that the monopole-corrected effective interactions used in the present calculations are reliable and can be employed for predictions of the properties of exotic nuclei in the region of ^{78}Ni. A systematic shell-model study of $N = 52$ and $N = 54$ nuclei is presented in Ref. [42].

ACKNOWLEDGMENTS

The authors would like to thank M. P. Carpenter, R. V. F. Janssens, F. G. Kondev, T. Lauritsen, C. J. Lister, and D. Seweryniak of the Physics Division of Argonne National Laboratory for their help in preparing and running the Gammasphere measurement. This work was partially supported by the US Department of Energy, Office of Nuclear Physics, under Contract No. DE-AC02-06CH11357. The authors are indebted for the use of ^{248}Cm to the Office of Basic Energy Sciences, Department of Energy, through the transplutonium element production facilities at Oak Ridge National Laboratory.

[1] J. Dobaczewski, I. Hamamoto, W. Nazarewicz, and J. A. Sheikh, Phys. Rev. Lett. **72**, 981 (1994).
[2] K. Sieja and F. Nowacki, Phys. Rev. C **81**, 061303(R) (2010).
[3] K. Sieja and F. Nowacki, Phys. Rev. C **85**, 051301(R) (2012).
[4] K. Sieja, F. Nowacki, K. Langanke, and G. Martínez-Pinedo, Phys. Rev. C **79**, 064310 (2009).
[5] T. Rząca-Urban, K. Sieja, W. Urban, F. Nowacki, J. L. Durell, A. G. Smith, and I. Ahmad, Phys. Rev. C **79**, 024319 (2009).
[6] G. S. Simpson, W. Urban, K. Sieja, J. A. Dare, J. Jolie, A. Linneman, R. Orlandi, A. Scherillo, A. G. Smith, T. Soldner, I. Tsekhanovich, B. J. Varley, A. Złomaniec, J. L. Durell, J. F. Smith, T. Rząca-Urban, H. Faust, I. Ahmad, and J. P. Greene, Phys. Rev. C **82**, 024302 (2010).
[7] W. Urban, K. Sieja, G. S. Simpson, H. Faust, T. Rząca-Urban, A. Złomaniec, M. Łukasiewicz, A. G. Smith, J. L. Durell, J. F. Smith, B. J. Varley, F. Nowacki, and I. Ahmad, Phys. Rev. C **79**, 044304 (2009).
[8] W. M. Alberico, A. De Pace, G. Garbarino, and A. Ramos, Phys. Rev. C **61**, 044314 (2000).
[9] E. F. Jones, P. M. Gore, J. H. Hamilton, A. V. Ramayya, J. K. Hwang, A. P. de Lima, S. J. Zhu, C. J. Beyer, Y. X. Luo, W. C. Ma *et al.*, Phys. Rev. C **73**, 017301 (2006).
[10] T. Rząca-Urban, W. Urban, A. Kaczor, J. L. Durell, M. J. Leddy, M. A. Jones, W. R. Phillips, A. G. Smith, B. J. Varley, I. Ahmad *et al.*, Eur. Phys. J. A **9**, 165 (2000).
[11] K. Li, J. H. Hamilton, A. V. Ramayya, S. H. Liu, X. Q. Zhang, N. T. Brewer, J. K. Hwang, C. Goodin, S. J. Zhu, Y. X. Luo, J. O. Rasmussen *et al.*, Int. J. Mod. Phys. E **20**, 1825 (2011).
[12] P. J. Nolan, F. A. Beck, and D. B. Fossan, Annu. Rev. Nucl. Part. Sci. **44**, 561 (1994).
[13] W. Urban, J. L. Durell, W. R. Phillips, A. G. Smith, M. A. Jones, I. Ahmad, A. R. Barnett, M. Bentaleb, S. J. Dorning, M. J. Leddy *et al.*, Z. Phys. A **358**, 145 (1997).
[14] D. Patel, A. G. Smith, G. S. Simpson, R. M. Wall, J. F. Smith, O. J. Onakanmi, I. Ahmad, J. P. Greene, M. P. Carpenter, T. Lauritsen *et al.*, J. Phys. G **28**, 649 (2002).
[15] T. Rząca-Urban, W. Urban, A. G. Smith, I. Ahmad, and A. Syntfeld-Każuch, Phys. Rev. C **87**, 031305(R) (2013).
[16] W. Urban, W. Kurcewicz, A. Nowak, T. Rząca-Urban, J. L. Durell, M. J. Leddy, M. A. Jones, W. R. Phillips, A. G. Smith, B. J. Varley *et al.*, Eur. Phys. J. A **5**, 239 (1999).

[17] A. G. Smith, J. L. Durell, W. R. Phillips, M. A. Jones, M. Leddy, W. Urban, B. J. Varley, I. Ahmad, L. R. Morss *et al.*, Phys. Rev. Lett. **77**, 1711 (1996).
[18] M. Czerwiński *et al.* (unpublished).
[19] M. A. Jones, W. Urban, and W. R. Phillips, Rev. Sci. Instrum. A **69**, 41209 (1998).
[20] W. Urban, M. Jentschel, B. Märkisch, Th. Materna, Ch. Bernards, C. Drescher, Ch. Fransen, J. Jolie, U. Köster, P. Mutti, T. Rząca-Urban, and G. S. Simpson, JINST **8**, P03014 (2013).
[21] I. Ahmad and W. R. Phillips, Rep. Prog. Phys. **58**, 1415 (1995).
[22] G. Mukherjee and A. A. Sonzogni, Nucl. Data Sheets **105**, 419 (2004).
[23] T. Rząca-Urban, W. Urban, J. L. Durell, A. G. Smith, and I. Ahmad, Phys. Rev. C **76**, 027302 (2007).
[24] E. A. Stefanova, R. Schwengner, G. Rainovski, K. D. Schilling, A. Wagner, F. Dönau, E. Galindo, A. Jungclaus, K. P. Lieb, O. Thelen, J. Eberth, D. R. Napoli, C. A. Ur, G. de Angelis, M. Axiotis, A. Gadea, N. Marginean, T. Martinez, T. Kroll, and T. Kutsarova, Phys. Rev. C **63**, 064315 (2001).
[25] C. M. Baglin, Nuclear Data Sheets **113**, 2187 (2012).
[26] D. Abriola and A. A. Sonzogni, Nucl. Data Sheets **107**, 2423 (2006).
[27] D. Abriola and A. A. Sonzogni, Nucl. Data Sheets **109**, 2501 (2008).
[28] P. Federman and S. Pittel, Phys. Lett. B **69**, 385 (1977); **77**, 29 (1978); Phys. Rev. C **20**, 820 (1979).
[29] P. Federman, S. Pittel, and R. Campos, Phys. Lett. B **82**, 9 (1979).
[30] W. Urban, M. Jentschel, R. F. Casten, J. Jolie, Ch. Bernards, B. Märkisch, Th. Materna, P. Mutti, L. Próchniak, T. Rząca-Urban *et al.*, Phys. Rev. C **87**, 031304(R) (2013).
[31] E. Caurier and F. Nowacki, Acta Phys. Pol. B **30**, 705 (1999).
[32] E. Caurier, G. Martinez-Pinedo, F. Nowacki, A. Poves, and A. P. Zuker, Rev. Mod. Phys. **77**, 427 (2005).
[33] J. Kurpeta, W. Urban, A. Plochocki, J. Rissanen, V.-V. Elomaa, T. Eronen, J. Hakala, A. Jokinen, A. Kankainen, P. Karvonen *et al.*, Phys. Rev. C **82**, 027306 (2010).
[34] J. Kurpeta, J. Rissanen, A. Plochocki, W. Urban, V.-V. Elomaa, T. Eronen, J. Hakala, A. Jokinen, A. Kankainen, P. Karvonen *et al.*, Phys. Rev. C **82**, 064318 (2010).
[35] K. Heyde and J. L. Wood, Rev. Mod. Phys. **83**, 1467 (2011).
[36] S. Raman, C. W. Nestor Jr., and P. Tikkanen, At. Data Nucl. Data Tables **78**, 1 (2001).
[37] Y. B. Wang, J. Rissanen, Hyperfine Interact. (2012).
[38] Y. H. Zhang, Zs. Podolyak, G. de Angelis, A. Gadea, C. Ur, S. Lunardi, N. Marginean, C. Rusu, R. Schwengner, Th. Kröll, D. R. Napoli, R. Mengazzo, D. Bazzacco *et al.*, Phys. Rev. C **70**, 024301 (2004).
[39] A. Astier, M.-G. Porquet, Ts. Venkova, I. Deloncle, A. Azaiez, A. Buta, D. Curien, O. Dorvaux, G. Duchene, B. J. P. Gall *et al.*, Eur. Phys. J. A **30**, 541 (2006).
[40] A. Gade, T. Baugher, D. Bazin, B. A. Brown, C. M. Campbell, T. Glasmacher, G. F. Grinyer, M. Honma *et al.*, Phys. Rev. C **81**, 064326 (2010).
[41] M.-G. Porquet and O. Sorlin, Phys. Rev. C **85**, 014307 (2012).
[42] K. Sieja, T. R. Rodriguez, K. Kołos, and D. Verney, Phys. Rev. C **88**, 034327 (2013).